

# Modeling lossy propagation of non-classical light

Ulvi Yurtsever\*

*MathSense Analytics, 1273 Sunny Oaks Circle, Altadena, CA 91001 and  
Hearne Institute for Theoretical Physics, Louisiana State University, Baton Rouge, LA 70803*

(Dated: December 1, 2018)

The lossy propagation law (generalization of Lambert-Beer's law for classical radiation loss) for non-classical, dual-mode entangled states is derived from first principles, using an infinite-series of beam splitters to model continuous photon loss. This model is general enough to accommodate stray-photon noise along the propagation, as well as amplitude attenuation. An explicit analytical expression for the density matrix as a function of propagation distance is obtained for completely general input states with bounded photon number in each mode. The result is analyzed numerically for various examples of input states. For N00N state input, the loss of coherence and entanglement is super exponential as predicted by a number of previous studies. However, for generic input states, where the coefficients are generated randomly, the decay of coherence is very different; in fact no worse than the classical Beer-Lambert law. More surprisingly, there is a plateau at a mid-range interval in propagation distance where the loss is in fact sub-classical, following which it resumes the classical rate. The qualitative behavior of the decay of entanglement for two-mode propagation is also analyzed numerically for ensembles of random states using the behavior of negativity as a function of propagation distance.

PACS numbers: 03.65.Ta, 06.20.Dk, 42.50.Lc, 42.50.St

We will derive the quantum analogue of the classical Beer-Lambert law for lossy propagation [1] from first principles by modeling the propagation medium as a continuum series of linear optical scattering elements. The results we report here suggest that the super-exponential propagation loss behavior of N00N states is highly special, and not likely to be shared by generic entangled states in the larger Hilbert space of the dual photon channel. The intuition that entanglement embedded in a general state would decay similarly to the decay of entanglement in the lossy propagation of a N00N state appears to be faulty. Assuming even part of the coherent entanglement that survives during the propagation of a generic entangled state can be utilized to produce super-classical phase sensitivity using an appropriate detection scheme [2], there appear to be many candidate states which are both robust against decoherence and non-classical enough to achieve significant advantage over classical light in an optimized quantum sensor architecture. This is consistent with and a generalization of previous results involving m-and-m states [3].

The basic model is illustrated in Figure 1. Here we first analyze the propagation of single-mode quantum light. The model assumes a series of  $M$  identical beam splitters into which that the input modes are  $a_0, d_1, d_2, \dots, d_M$ , where  $a_0$  is the incoming photon mode, and  $d_1, d_2, \dots, d_M$  are auxiliary channels possibly populated by stray light or thermal photons, but for the discussion here we will assume these channels have vacuum inputs. Similarly, the output modes are  $a_M, s_1, s_2, \dots, s_M$ , where  $a_M$  is the output photon mode corresponding to the input channel  $a_0$ , and  $s_1, s_2, \dots, s_M$  are auxiliary channels modeling scattered and absorbed light along the propagation medium. The idea is to let the number of beam splitters  $M$  approach infinity in a controlled manner at the end of the calculation to extract the loss behavior of the quantum state propagating non-unitarily from the  $a_0$  channel to the  $a_M$  channel.

At each beam splitter  $k$  in Fig. 1, unitarity requires the relations

$$\begin{aligned} a_k &= T a_{k-1} + L d_k, \\ s_k &= L a_{k-1} + T d_k, \quad k = 1, 2, \dots, M, \end{aligned} \tag{1}$$

where  $T$  and  $L$  are the complex transmission and reflection coefficients and satisfy the unitarity conditions

$$\begin{aligned} |L|^2 + |T|^2 &= 1 \\ L \bar{T} + T \bar{L} &= 0 \end{aligned} \tag{2}$$

---

\*Electronic address: ulvi@phys.lsu.edu

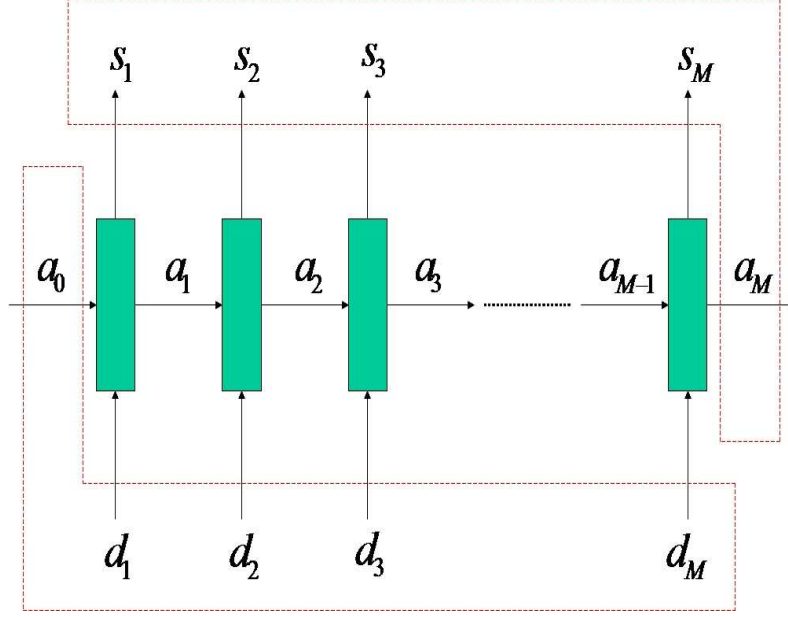


**FIG. 1:** Diagram illustrating the series-of-beam-splitters model for propagation loss.

In terms of the creation operators  $a_k^\dagger$ ,  $d_k^\dagger$ , and  $s_k^\dagger$ , Eqs. (1) can be rewritten in the form

$$\begin{aligned} a_k^\dagger &= \bar{T} a_{k-1}^\dagger + \bar{L} d_k^\dagger, \\ s_k^\dagger &= \bar{L} a_{k-1}^\dagger + \bar{T} d_k^\dagger, \quad k = 1, 2, \dots, M, \end{aligned} \quad (3)$$

The input and output modes are connected by a unitary transformation that can be written in the form of a linear map

$$\begin{bmatrix} a_0^\dagger \\ d_1^\dagger \\ d_2^\dagger \\ d_3^\dagger \\ \vdots \\ d_M^\dagger \end{bmatrix} = U \begin{bmatrix} a_M^\dagger \\ s_1^\dagger \\ s_2^\dagger \\ s_3^\dagger \\ \vdots \\ s_M^\dagger \end{bmatrix}. \quad (4)$$

Using Eqs. (3), the  $(M+1) \times (M+1)$  unitary matrix  $U$  can be written explicitly in terms of the reflection and transmission coefficients of the beam splitters:

$$U = \begin{bmatrix} T^M & L & LT & LT^2 & \dots & LT^{M-1} \\ LT^{M-1} & T & L^2 & L^2 T & \dots & L^2 T^{M-2} \\ LT^{M-2} & 0 & T & L^2 & \dots & L^2 T^{M-3} \\ LT^{M-3} & 0 & 0 & T & \dots & L^2 T^{M-4} \\ \vdots & \vdots & \vdots & \vdots & \ddots & \vdots \\ L & 0 & 0 & 0 & \dots & T \end{bmatrix}. \quad (5)$$

It can be checked by straightforward calculation that the unitarity relations Eqs. (2) imply

$$U^\dagger U = \mathbb{I} \quad (6)$$

Since by Eqs. (4)–(5)

$$a_0^\dagger = T^M a_M^\dagger + L s_1^\dagger + L T s_2^\dagger + L T^2 s_3^\dagger + \dots + L T^{M-1} s_M^\dagger, \quad (7)$$

an incoming number Fock-state purely in the input mode

$$|\psi_{\text{in}}\rangle = |N\rangle = \frac{1}{\sqrt{N!}}(a_0^\dagger)^N |0\rangle \quad (8)$$

is transformed to the outgoing state

$$|\psi_{\text{out}}\rangle = \frac{1}{\sqrt{N!}} \left( T^M a_M^\dagger + L s_1^\dagger + L T s_2^\dagger + L T^2 s_3^\dagger + \dots + L T^{M-1} s_M^\dagger \right)^N |0\rangle. \quad (9)$$

As mentioned before, Eq. (8) assumes that the auxiliary input modes  $\{d_1, d_2, \dots, d_M\}$  are vacuum ports. More generally, our model can accommodate noise in the form of stray photons leaking *into* the propagation channel by simply replacing the input state Eq. (8) with a state of the form

$$|\psi_{\text{in}}\rangle = \frac{1}{\sqrt{N!}} (a_0^\dagger)^N \sum_{q_1, q_2, \dots, q_M} c_{q_1, q_2, \dots, q_M} (d_1^\dagger)^{q_1} (d_2^\dagger)^{q_2} \dots (d_M^\dagger)^{q_M} |0\rangle \quad (8')$$

To handle incoherent (such as thermal) input noise, one would have to enlarge the Hilbert space of the auxiliary input modes  $\{d_1, d_2, \dots, d_M\}$  to include their own environment modes, and trace over these secondary environment modes at the end of the calculation [4].

Going back to the input number state in the form Eq. (8), we can calculate the final output state (density matrix) in the out-mode (whose creation operator is  $a_M^\dagger$ ) by tracing over the loss (scattering) modes  $s_1, s_2, \dots, s_M$ :

$$\rho_{\text{out}} = \text{Tr}_{\{s_1, s_2, \dots, s_M\}} |\psi_{\text{out}}\rangle \langle \psi_{\text{out}}|. \quad (10)$$

Substituting Eq. (9) for  $|\psi_{\text{out}}\rangle$ , this calculation gives

$$\rho_{\text{out}} = \sum_{\substack{n_0, \dots, n_M=0 \\ \sum_{\alpha=0}^M n_\alpha = N}}^N \frac{N!}{n_0! n_1! \dots n_M!} |T|^{2n_0 M} |T|^{2 \sum_{i=1}^M (i-1) n_i} |L|^{2 \sum_{i=1}^M n_i} |n_0\rangle_{s_0} \langle n_0|_{s_0}, \quad (11)$$

where, for ease of combinatorial manipulation, we renamed the output  $M$ -mode with index 0:  $s_0 \equiv a_M$  (equivalently,  $s_0^\dagger = a_M^\dagger$ ), and  $|k\rangle_{s_0} \equiv |k\rangle_{s_M}$ . It is convenient to combinatorially manipulate Eq. (11) and rewrite it in the following form

$$\rho_{\text{out}} = \sum_{n_0=0}^N \frac{N!}{n_0! (N-n_0)!} |n_0\rangle_{s_0} \langle n_0|_{s_0} \sum_{\substack{n_1, \dots, n_M=0 \\ \sum_{j=1}^M n_j = N-n_0}}^N \frac{(N-n_0)!}{n_1! n_2! \dots n_M!} |T|^{2n_0 M} |T|^{2 \sum_{i=1}^M (i-1) n_i} |L|^{2 \sum_{i=1}^M n_i}. \quad (12)$$

The continuum limit is defined by taking the number of beam splitters  $M$  to infinity, while keeping the “power lost” per unit length of propagation constant. Since each beam-splitter’s contribution to power loss is given by  $|L|^2$ , mathematically this amounts to the limiting process (Fig. 2)

$$\text{Limit process for amplitude evolution: } \begin{cases} M \rightarrow \infty \\ L \rightarrow 0 \\ |L|^2 \frac{M}{x} \rightarrow \text{constant} \equiv \mu \\ |T|^{2M} = (1 - |L|^2)^M \rightarrow \left(1 - \frac{\mu x}{M}\right)^M \rightarrow e^{-\mu x} \end{cases} \quad (13)$$

Similarly, to preserve unitarity, a corresponding limit process must govern the evolution of the “phase”  $\eta$  of the complex transmission amplitude  $T$ :

$$\text{Limit process for phase evolution: } \begin{cases} M \rightarrow \infty \\ T \equiv |T| e^{i\phi} \\ \phi \rightarrow 0 \\ \phi \frac{M}{x} \rightarrow \text{constant} \equiv \eta \\ T^M \rightarrow |T|^M e^{i\eta x} \end{cases} \quad (14)$$

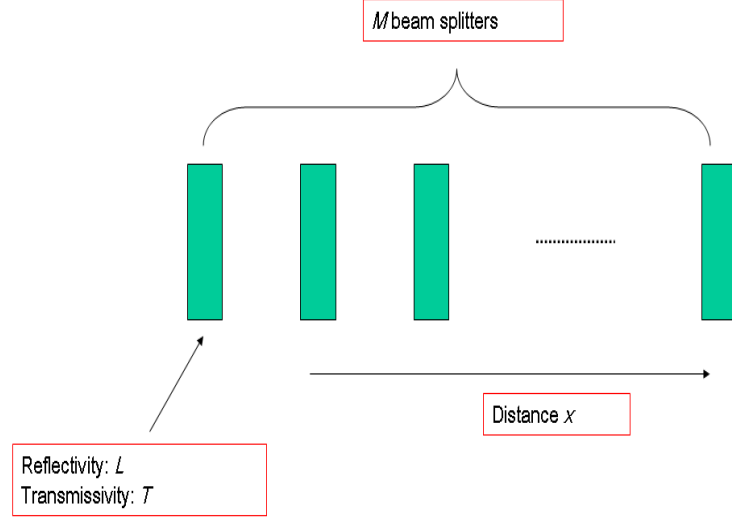


**FIG. 2:** The “Beer” limiting process where discrete beam splitters merge into a continuous propagation medium.

Substituting Eqs. (13) and (14) into Eq. (12) yields our sought-for result for the  $x$ -dependent output density matrix resulting from an input Fock number state with  $N$  photons:

$$\rho_{\text{out}}(x) = \sum_{n=0}^N \binom{N}{n} e^{-n\mu x} (1 - e^{-\mu x})^{N-n} |n\rangle\langle n|. \quad (15)$$

The interpretation of Eq. (15) in terms of photon loss as a function of propagation distance is straightforward (see also [5] for an alternate derivation with a fixed amount of loss).

Let’s now turn to the analysis of dual-channel lossy propagation. We proceed similarly to the single-mode case, and adopt the notation for labeling the input, output, and scattering modes as illustrated by Fig. 3. Everything in the analysis above between Eqs. (1) and (7) proceeds independently for the two propagation channels  $a$  and  $b$ , with corresponding series of beam splitters having in general distinct reflection and transmission characteristics. The dual-channel version of Eq. (7) is

$$\begin{aligned} a_0^\dagger &= T_a^M a_M^\dagger + L_a s_1^\dagger + L_a T_a s_2^\dagger + L_a T_a^2 s_3^\dagger + \cdots + L_a T_a^{M-1} s_M^\dagger \\ b_0^\dagger &= T_b^M b_M^\dagger + L_b t_1^\dagger + L_b T_b t_2^\dagger + L_b T_b^2 t_3^\dagger + \cdots + L_b T_b^{M-1} t_M^\dagger. \end{aligned} \quad (16)$$

As a first, important example, consider an input N00N state which has the form

$$|\psi_{\text{in}}\rangle = \frac{1}{\sqrt{2}} (|N\rangle_a |0\rangle_b + |0\rangle_a |N\rangle_b) = \frac{1}{\sqrt{2N!}} \left( (a_0^\dagger)^N + (b_0^\dagger)^N \right) |0\rangle_a |0\rangle_b. \quad (17)$$

According to Eq. (16), the output state is given by

$$\begin{aligned} |\psi_{\text{out}}\rangle &= \frac{1}{\sqrt{2N!}} \left[ \left( T_a^M a_M^\dagger + L_a s_1^\dagger + L_a T_a s_2^\dagger + L_a T_a^2 s_3^\dagger + \cdots + L_a T_a^{M-1} s_M^\dagger \right)^N \right. \\ &\quad \left. + \left( T_b^M b_M^\dagger + L_b t_1^\dagger + L_b T_b t_2^\dagger + L_b T_b^2 t_3^\dagger + \cdots + L_b T_b^{M-1} t_M^\dagger \right)^N \right] |0\rangle_a |0\rangle_b. \end{aligned} \quad (18)$$

As before, the output density matrix is obtained by tracing over the scattering modes:

$$\rho_{\text{out}} = \text{Tr}_{\{s_1, \dots, s_M, t_1, \dots, t_M\}} |\psi_{\text{out}}\rangle\langle\psi_{\text{out}}|. \quad (19)$$

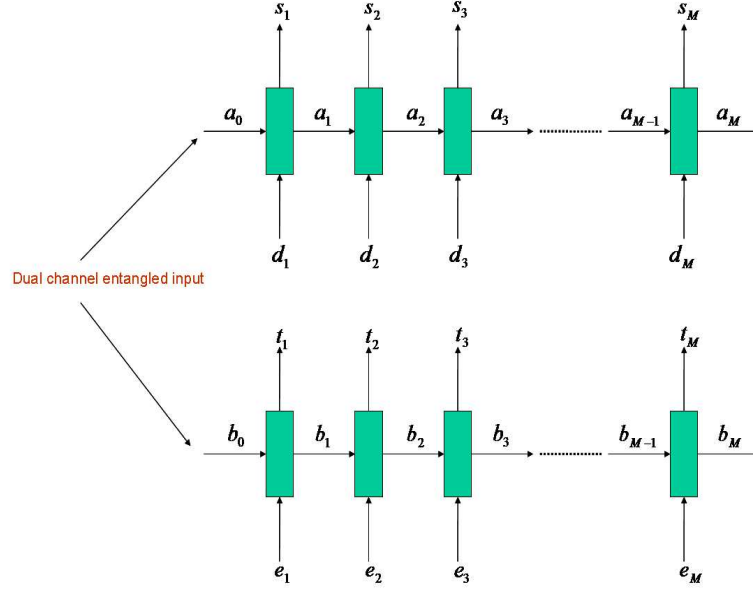


**FIG. 3:** Modeling propagation loss for dual-channel entangled photon states with a series of beam splitters.

Substituting Eq. (18) in Eq. (19) and carrying out some straightforward algebra, we reach the dual-channel analogue of Eq. (12), which we will suppress here to save space. Applying the Beer limit process ( $M \rightarrow \infty$ ) defined by Eqs. (13) and (14) to this expression (whereby each channel  $a, b$  is associated with its own version of the extinction and phase-rotation coefficients  $\mu_a, \mu_b, \eta_a$ , and  $\eta_b$ ) yields the following continuum limit for the output density matrix of a N00N input state as a function of propagation distance  $x$ :

$$\begin{aligned} \rho_{\text{out}}(x) = & \frac{1}{2} \left[ \sum_{n=0}^N \binom{N}{n} \left[ e^{-n\mu_a x} (1 - e^{-\mu_a x})^{N-n} |n\rangle_a |0\rangle_b \langle n|_a \langle 0|_b + e^{-n\mu_b x} (1 - e^{-\mu_b x})^{N-n} |0\rangle_a |n\rangle_b \langle 0|_a \langle n|_b \right] \right. \\ & \left. + e^{-\frac{N}{2}(\mu_a + \mu_b)x} \left( e^{i(\eta_a - \eta_b)x} |N\rangle_a |0\rangle_b \langle 0|_a \langle N|_b + e^{-i(\eta_a - \eta_b)x} |0\rangle_a |N\rangle_b \langle N|_a \langle 0|_b \right) \right]. \end{aligned} \quad (20)$$

Note that the coherence term is the entire expression on the second line of Eq. (20). This term is exponentially suppressed with an extinction coefficient given by  $N\mu$ , where  $\mu \equiv (\mu_a + \mu_b)/2$  is the average extinction coefficient of the two propagation channels. Hence the well-understood “super-exponential” loss of coherence (hence loss of entanglement) in the propagation of N00N states is once again verified [6].

After working through the N00N state example above, it is straightforward but rather cumbersome to extend our calculation to a completely general two-mode input state, the only restriction being that the maximum photon number  $N$  in each mode  $a$  and  $b$  is finite. This most general input state can be written in the form

$$|\psi_{\text{in}}\rangle = \sum_{l,m=0}^N \frac{\alpha_{lm}}{\sqrt{l!m!}} (a_0^\dagger)^l (b_0^\dagger)^m |0\rangle_a |0\rangle_b, \quad \sum_{l,m=0}^N |\alpha_{lm}|^2 = 1. \quad (21)$$

Straightforward calculation in the spirit of the analysis presented thus far gives the result

$$\begin{aligned} \rho_{\text{out}}(x_a, x_b) = & \sum_{l,m,l',m'=0}^N \alpha_{lm} \overline{\alpha_{l'm'}} e^{i(l-l')\eta_a x_a} e^{i(m-m')\eta_b x_b} e^{-\frac{1}{2}(l'-l)\mu_a x_a} e^{-\frac{1}{2}(m'-m)\mu_b x_b} \times \\ & \times \sum_{p=0}^l \sum_{q=0}^m \frac{1}{(l-p)!(m-q)!} \left( \frac{l! l'! m! m'!}{p! q! (p+l'-l)!(q+m'-m)!} \right)^{\frac{1}{2}} \times \\ & \times e^{-p\mu_a x_a} (1 - e^{-\mu_a x_a})^{l-p} e^{-q\mu_b x_b} (1 - e^{-\mu_b x_b})^{m-q} |p\rangle_a |q\rangle_b \langle p+l'-l|_a \langle q+m'-m|_b, \end{aligned} \quad (22)$$

where we also implemented a trivial generalization by allowing the output “point” to have different  $x$  coordinates  $x_a$  and  $x_b$  along the two distinct propagation paths. Here and in what follows we adopt the combinatorial convention that the factorial of a negative integer is  $+\infty$ ; thus the contributions to the above sum from, e.g., terms with  $l < p$  or  $p + l' < l$  vanish by virtue of the factorial terms in the denominator. A somewhat lengthy binomial-chase through the sums in Eq. (22) allows us to put it into the slightly more manageable alternative form:

$$\begin{aligned} \rho_{\text{out}}(x_a, x_b) &= \sum_{p, q, p', q'=0}^N |p\rangle_a |q\rangle_b \langle p'|_a \langle q'|_b \times \\ &\times e^{-\frac{1}{2}(p+p')\mu_a x_a} e^{-\frac{1}{2}(q+q')\mu_b x_b} e^{i(p-p')\eta_a x_a} e^{i(q-q')\eta_b x_b} \times \\ &\times \sum_{l=p}^N \sum_{m=q}^N \frac{\alpha_{lm} \overline{\alpha_{l+p'-p, m+q'-q}}}{(l-p)!(m-q)!} \left( \frac{l!(l+p'-p)! m!(m+q'-q)!}{p! q! p'! q'!} \right)^{\frac{1}{2}} \times \\ &\times (1 - e^{-\mu_a x_a})^{l-p} (1 - e^{-\mu_b x_b})^{m-q} . \end{aligned} \quad (23)$$

Before we begin analyzing the consequences of our main result Eq. (23) quantitatively, we mention one last generalization which is quite straightforward. It is easy to incorporate  $x$ -dependent (variable) extinction and phase rotation coefficients  $\mu$  and  $\eta$  into the above development merely via the substitutions in the limit process Eqs. (13)–(14)

$$\begin{aligned} e^{-\mu x} &\longrightarrow e^{-\int_0^x \mu(\zeta) d\zeta} \\ e^{i\eta x} &\longrightarrow e^{i \int_0^x \eta(\zeta) d\zeta} . \end{aligned} \quad (24)$$

With this generalization, the result Eq. (23) becomes

$$\begin{aligned} \rho_{\text{out}}(x_a, x_b) &= \sum_{p, q, p', q'=0}^N |p\rangle_a |q\rangle_b \langle p'|_a \langle q'|_b \times \\ &\times e^{-\frac{1}{2}(p+p') \int_0^{x_a} \mu_a} e^{-\frac{1}{2}(q+q') \int_0^{x_b} \mu_b} e^{i(p-p') \int_0^{x_a} \eta_a} e^{i(q-q') \int_0^{x_b} \eta_b} \times \\ &\times \sum_{l=p}^N \sum_{m=q}^N \frac{\alpha_{lm} \overline{\alpha_{l+p'-p, m+q'-q}}}{(l-p)!(m-q)!} \left( \frac{l!(l+p'-p)! m!(m+q'-q)!}{p! q! p'! q'!} \right)^{\frac{1}{2}} \times \\ &\times (1 - e^{-\int_0^{x_a} \mu_a})^{l-p} (1 - e^{-\int_0^{x_b} \mu_b})^{m-q} . \end{aligned} \quad (25)$$

We now calculate the decay of coherence and entanglement numerically using the above formalism for N00N and generic (random) entangled states. The main results are illustrated by the plots in Figs. 4–7.

All of our plots are generated assuming constant extinction and rotation coefficients  $\mu = \mu_a = \mu_b = 0.2 \text{ km}^{-1}$  and  $\eta = \eta_a = \eta_b = 1 \text{ km}^{-1}$ . The amount of coherence is calculated by computing the sum of absolute squares of the off-diagonal elements of the density matrix (the off-diagonal matrix norm squared); hence it can be interpreted as the coherence “power” that survives in the density matrix as it propagates through the lossy medium. Also note that in all three plots Figs. 4–7 the  $x$  axis is the propagation distance, and the  $y$ -axis depicts the logarithm of the dependent variable.

Fig. 4 makes clear the “super-exponential” decay of coherence for a N00N state as a function of propagation distance. For the  $N = 10$  N00N state, coherence power decays proportionally to  $\exp(-2N\mu x)$  as expected from Eq. (20).

In contrast to Fig. 4, Fig. 5 suggests an unexpected robustness of coherence in generic entangled states against propagation loss. Here we plot the coherence power as a function of propagation distance for two ensembles of entangled states, drawn randomly from two different probability distributions on the Hilbert space of all states of the form Eq. (21). One ensemble is drawn from a joint uniform distribution for the real and imaginary parts of  $\alpha_{ij}$ , which is then normalized. The other ensemble is drawn from a true uniform distribution on the Bloch sphere in the complex space  $\mathbb{C}^{N+1}$ . To generate the latter ensemble, we utilize the result that  $(z_1, \dots, z_n)/\sqrt{|z_1|^2 + \dots + |z_n|^2}$  is a random vector on the unit sphere  $S^{2n-1}$  in  $\mathbb{C}^n$  with respect to the canonical volume form on  $S^{2n-1}$  if  $\text{Re}(z_i)$ ,  $\text{Im}(z_j)$  are i.i.d. Gaussian random variables with zero mean [7, 8]. We see from Fig. 5 that:

- For a random entangled input state, coherence decays no faster than the classical loss rate.

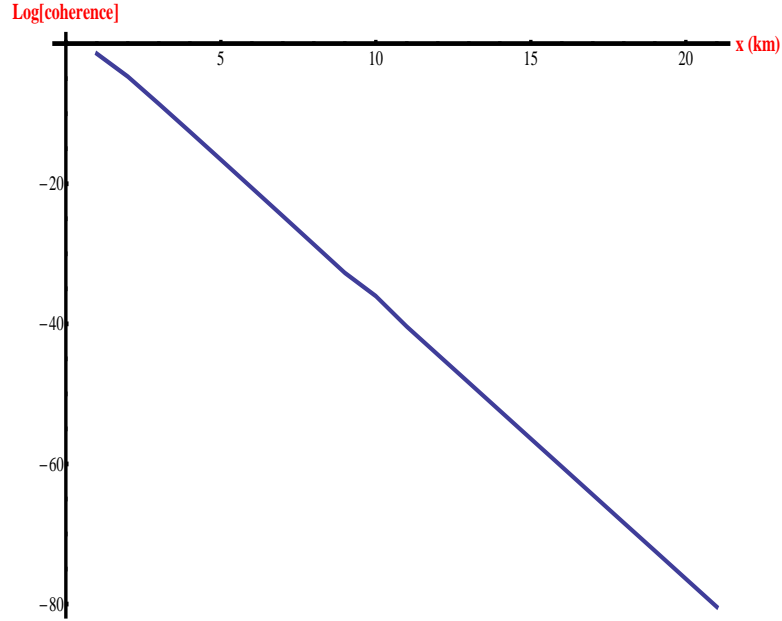


**FIG. 4:** Decay behavior of coherence power (the sum of absolute squares of the off-diagonal elements) for a  $N = 10$  N00N state.

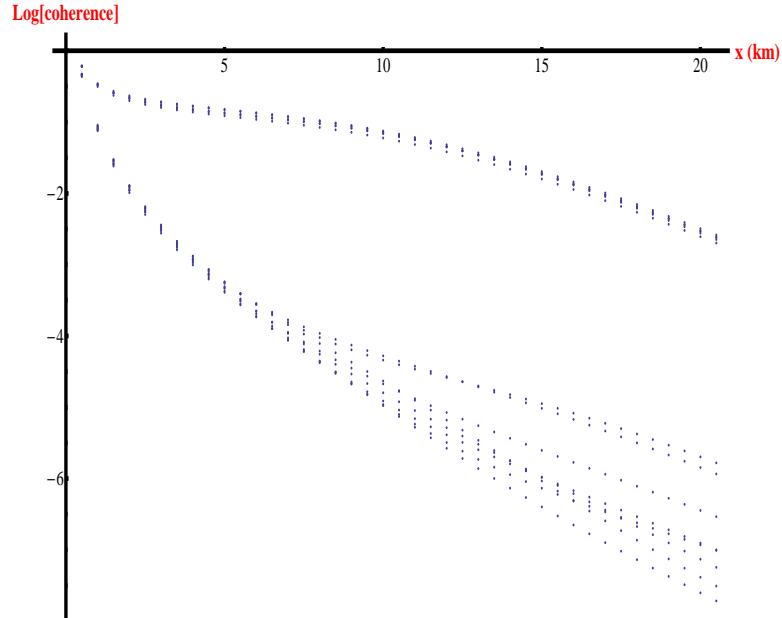


**FIG. 5:** Decay of coherence power for two ensembles of random entangled states (Eq. (21)) with  $N = 10$ . Note the slight plateau in decay at medium propagation distances. The plateau reverts back to exponential decay at large propagation distances; however, the overall decay remains no worse than that of classical light. The upper ensemble is drawn from a joint uniform distribution for the real and imaginary parts of  $\alpha_{ij}$ , which is then normalized. The lower ensemble is drawn from a true uniform distribution on the Bloch sphere in the complex space  $\mathbb{C}^{N+1}$ , where here  $N = 10$ .

- There is a mid-range plateau in loss, where decay is sub-classical, after which classical decay-rate resumes. This feature is present for all generic entangled inputs.
- How much of the surviving generic coherence is useful for super-classical resolution will depend more on the survival rate of entanglement than on that of coherence.

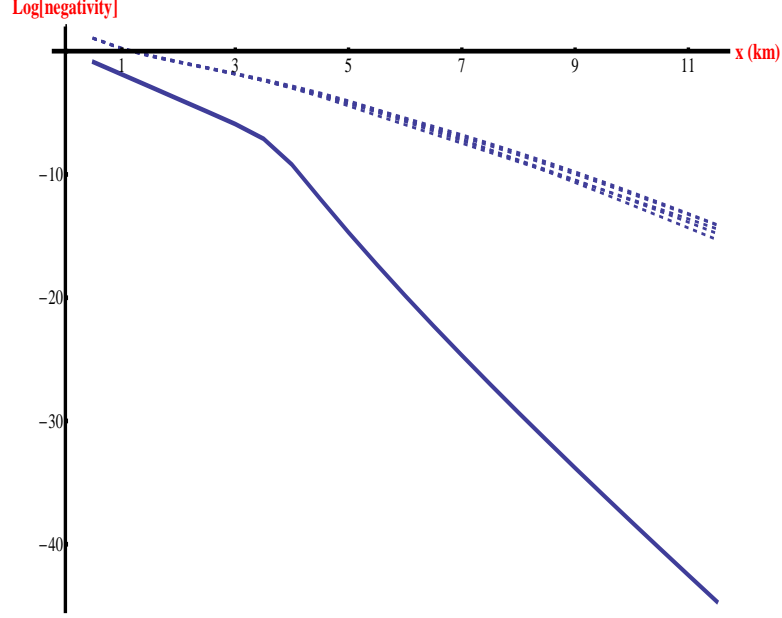


**FIG. 6:** Behavior of negativity for the  $N = 10$  N00N state and a random ensemble of entangled states ( $N = 10$ ). The ensemble is drawn from a true uniform distribution on the Bloch sphere in the complex space  $\mathbb{C}^{N+1}$  as in Fig. 5.

To investigate the decay of entanglement in the density matrix that results from the propagation of a generic input state of the form Eq. (21), we use the concept of “negativity” [9, 10]. Consider a mixed state of a general bi-partite system with Hilbert space  $\mathcal{H}_A \otimes \mathcal{H}_B$  given by

$$\rho = \sum_{i,j,k,l} \rho_{ij,kl} |i_A j_B\rangle \otimes \langle k_A l_B|, \quad (26)$$

where  $\{|i_A j_B\rangle\}$  is a separable orthonormal basis for  $\mathcal{H}_A \otimes \mathcal{H}_B$ . The “partial transpose” of  $\rho$  with respect to the subsystem  $A$  is defined as the operator

$$\rho^{t_A} \equiv \sum_{i,j,k,l} \rho_{kj,il} |i_A j_B\rangle \otimes \langle k_A l_B|. \quad (27)$$

Although the partial transpose  $\rho^{t_A}$  is symmetric and has unit trace, it is in general not a density matrix since it is not necessarily a positive operator. In fact, the separability of  $\rho$  is a sufficient (though not necessary) condition for the positivity of  $\rho^{t_A}$ . In other words, the negativity of  $\rho^{t_A}$  guarantees entanglement, but it is not necessary that  $\rho^{t_A}$  is negative for entanglement to be present. This makes negativity a partial entanglement measure which is relatively easy to compute. Quantitatively, negativity is defined to be the (non-negative) quantity

$$\sum_{i: \lambda_i^{t_A} < 0} |\lambda_i^{t_A}|, \quad (28)$$

where the sum is over all eigenvalues of  $\rho^{t_A}$  which are negative.



In Fig. 6 we illustrate the behavior of negativity as a function of propagation distance for a N00N state and for a random ensemble of entangled states drawn randomly from the uniform probability distribution on the Bloch sphere in the Hilbert space of all states of the form Eq. (21). (See [11] for a different look at the behavior of entanglement under loss.)

It is apparent that the “super-exponential” propagation loss behavior of N00N states is a highly special property not shared by more general two-mode entangled non-classical states of light. Whether the latent robust entanglement of generic two-mode states illustrated in Fig. 6 can be used to reach super-classical resolution in metrology applications depends on what detection schemes can be deployed on the output density matrix [12], as well as, from a practical point of view, on whether the generic states can be created reproducibly. These are questions we will investigate in a forthcoming paper [4].

### Acknowledgments

I am grateful to Gabriel Durkin for useful correspondence on the quantitative description of entanglement in mixed states. The research work reported on in this paper was carried out with support from the Defense Advanced Research Project Agency. The views, opinions, and findings contained in this article are those of the author and should not be interpreted as representing the official views or policies, either expressed or implied, of the Defense Advanced Research Projects Agency or the Department of Defense.

- 
- [1] See L. Mandel and E. Wolf, *Optical Coherence and Quantum Optics* (Cambridge, Cambridge University Press, 1995), Sec. 5.7.4.
  - [2] J. P. Dowling, *Contemporary Physics* **49** (2) 125-143 (2008).
  - [3] D. B. Uskov, L. Kaplan, A. M. Smith, S. D. Huver, and J. P. Dowling, *Phys. Rev. A* **79**, 042326 (2009).
  - [4] U. Yurtsever, in preparation.
  - [5] G. A. Durkin, PhD Thesis, University of Oxford (2004).
  - [6] G. Gilbert, M. Hamrick, and Y. S. Weinstein, *JOSA B* **25**:8, 1336-1340 (2008).
  - [7] G. Marsaglia, *Ann. Math. Stat.* **43**, 645-646 (1972).
  - [8] E. Muller, *Comm. Assoc. Comput. Mach.* **2**, 19-20 (1959).
  - [9] G. Jaeger, *Quantum Information* (Springer-Verlag, 2007).
  - [10] M. A. Nielsen and I. L. Chuang, *Quantum Computing and Quantum Information* (Cambridge University Press, Cambridge, 2000).
  - [11] G. A. Durkin, C. Simon, J. Eisert, D. Bouwmeester, *Phys. Rev. B* **70**, 062305 (2004).
  - [12] R. Demkowicz-Dobrzanski et. al., *Quantum phase estimation with lossy interferometers*, available online at <http://xxx.lanl.gov/abs/0904.0456> (2009).